ISSN 0001-4338, Izvestiya, Atmospheric and Oceanic Physics, 2020, Vol. 56, No. 12, pp. 1482–1491. © Pleiades Publishing, Ltd., 2020.
Russian Text © The Author(s), 2020, published in Issledovanie Zemli iz Kosmosa, 2020, No. 3, pp. 14–25.

USING SPACE-BASED INFORMATION ABOUT THE EARTH SPACE MONITORING OF WILDFIRES, THEIR CONSEQUENCES, AND FOREST ECOSYSTEMS

Determining the Post-Fire State of Vegetation on the Territory of Ivano–Arakhley Nature Park (Zabaikal'sky Krai) Using Radar Sentinel 1 and Optical Sentinel 2 Data

N. V. Rodionova[a], *, I. L. Vakhnina[b], and T. V. Zhelibo[b]

[a]*Kotelnikov Institute of Radioengineering and Electronics, Fryazino Branch, Russian Academy of Sciences, Fryazino, Moscow Region, 141190 Russia*

[b]*Institute of Natural Resources, Ecology, and Cryology, Siberian Branch, Russian Academy of Sciences, Chita, 672090 Russia*

**e-mail: rnv@ire.rssi.ru*

Received January 29, 2020; revised March 3, 2020; accepted March 17, 2020

Abstract—Results are presented from an analysis of multitemporal data obtained via satellite monitoring of the state of vegetation on the territory of Ivano–Arakhley Nature Park (Zabaikal'sky krai) after a 2015 natural fire. Radar and optical data are acquired from the Sentinel 1 and Sentinel 2 spacecraft, respectively. Spectral indices NDVI, NBR, MIRBI, and NDRE are used in combination with radar vegetation index RVI to determine the dynamics of the restoration of the vegetation cover affected by the fire. The positive dynamics in the state of the vegetation in postfire period 2016–2019 is shown by an increase in the values of the NDVI, NBR, NDRE, and RVI indices. The effect the atmosphere on the values of the vegetation index is shown.

Keywords: C-band radar data, multispectral optical data, vegetation cover, wildfires, vegetation indices

DOI: 10.1134/S0001433820120518

INTRODUCTION

One of the highest levels of fire activity in Siberia is observed in Zabaikal'sky krai, where the climate is strongly continental and permafrost is always present. The ground freezes deeply to 1–1.5 m and thaws slowly. The restoration of vegetation is greatly hampered, due to low amounts of precipitation, 90% of which (within 300 mm) falls in the warm period, mainly in July and August. Winters have little snow, and the soil is not moistened by it. This results in the region being very much on fire in the spring. Researchers (Shvetsov et al., 2019) have found that a number of factors hinder the successful renewal of the Trans-Bailkal forest: (1) high soil temperatures on burned-out areas that dry out young trees; (2) lack of moisture and nutrients resulting in fierce competition between plants and the overgrowth of grass; and (3) repeated fires. Earth remote sensing and ground data are used to monitor the state of the forest after a fire.

Ground-based studies of the state of woody vegetation in the Ivano–Arakhley Nature Park were performed in 2013–2014 after ground fires in 2000, 2001, 2003, and 2010 (Gorbunov et al., 2015). Test sites established on the southeastern slopes of Osinovyi Ridge had typical types of forest foliage: rhododendra, lingonberry, and yernik. These stands of trees were susceptible to ground fires of varying intensity. The studies showed the natural regeneration of tree species was unsatisfactory.

In mid-April 2015, strong forest fires were observed in the Trans-Baikal region in the area of the Beklemishevskaya system of lakes on the territory of Ivano–Arakhley Nature Park. Figure 1a shows a map of fires in this area for April 14, 2015, according to data from the Kosmosnimki Fire Service's SCANEX operational monitoring system (http://fires.kosmosnimki.ru). Burned areas in this region were identified using amplitude and texture information obtained from radar images of the Sentinel 1 (S1) satellite (Rodionova, 2016).

After 2015, the territories of Ivano–Arakhley Nature Park were not exposed to fire for another four years.

In this work, we use radar and optical data from the Sentinel 1 and 2 satellites to follow the recovery of the vegetation on the territory of Ivano–Arakhley Nature Park for four years after the fire in 2015.

CHARACTERISTICS OF THE RESEARCH SITES

In the mountain–taiga larch landscapes of the Kondinsky steppe–depression district, model sites were identified to studying the dynamics of changes in plant communities (Fig. 1b). The site on Osinovy Ridge in the basin of the Osinovka River was conven-

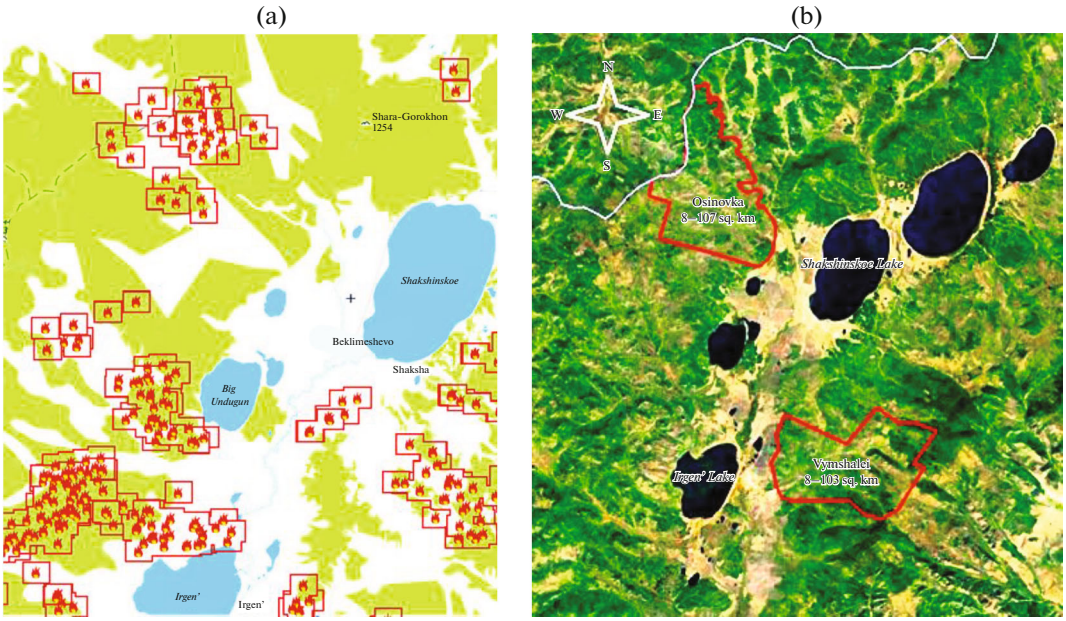

Fig. 1. (a) Map of fires for April 14, 2015, and (b) locations of model sites for studying the dynamics of changes in plant communities.

tionally denoted *Osinovka*, while a site on Yablonovy Ridge in the basin of the Ryshmaley river was named *Ryshmaley*. Detailed descriptions of the sites in Osinovka are given in Table 1, along with photographs of the test sites on which the study of 2018 was performed by the staff of the Institute of Natural Resources, Ecology, and Cryology in Chita.

In this work, 12 of 49 sites with numbers 3, 13, 16, 19, 20, 41, 42, 46, 52, 53, 71, and 72 were selected in Osinovka on territories that burned after the fires of 2015.

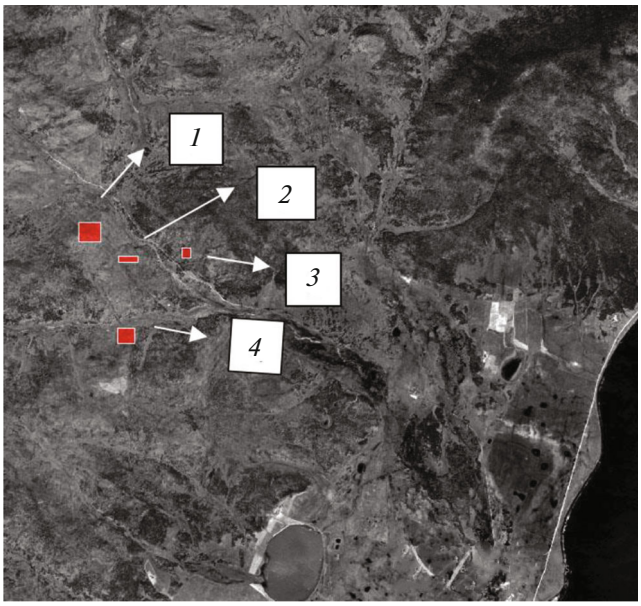

Fig. 2. Locations of the four groups of test sites.

Figure 2 shows the Sentinel 2 (S2) image of the studied area on July 31, 2018. The red rectangles mark the location of the test sites combined into four groups: (1) sites 20, 52, 53, 72; (2) sites 19 and 71; (3) sites 3 and 13; and (4) sites 41, 42, and 46. Site 16 is located between groups (3) and (4).

DATA AND PROCEDURES

Initial Sentinel 1 Radar Data. Radar Vegetation Index

In this work, we used open available Sentinel 1 radar data of the C-band of IW (interferometric wide swath) modes with VV and VH polarization and a spatial resolution of 10 m. The S1 images were processed using the SNAP program (https://sentinel.esa.int/web/sentinel/toolboxes/sentinel-1). Preliminary data processing included selecting a fragment with the studied site and radiometric calibration.

To determine the mean value along the profile of the backscattering coefficient (BSC) for the 12 studied sites, we used the S1 images from July 26, 2017, August 2, 2018, and July 28, 2019. To compare them to sites with burned-out areas, we chose a background site in the northern part of Shaksha Lake where there was no fire in 2015 (profile coordinates, 52.2037° N, 112.7229° E). Figure 3a shows a graph of the change in the BSC in dB for 12 sites and the background profile for 2017–2019. The plots were numbered along the abscissa in groups of 1 to 4, followed by site 16 and the background site. The BSC values grew for both polarizations over the period of 2017–2019 for all test sites. The greatest changes in the BSC were noted for VH cross polarization. For site 20, these were 6.6 dB over

Table 1. Description of test sites in Osinovka

No.	Coordinates	Height, m	Type of community	Disturbance of territory	Photo
3	52.20855° N, 112.56738° E	1070		Cutting burnt	
13	52.20631°, 112.56490°	1029	Cereal yernik	Burnt	
16	52.19739°, 112.57023°	996	Herb foliage	Gorelnic, windfall	
19	52°12′24,9″, 112°32′40,3″	1053	Lingonberry foliage	Burnt, windfall	
20	52°12′42,0″, 112°32′02,5″	1099	Lingonberry foliage	Burnt, windfall	
41	52.18975°, 112.54653°	1051	Herb foliage	Burnt, windfall	
42	52.19275°, 112.54384°	1021	Herb foliage	Burnt	
46	52.19133°, 112.54929°	1066	The listvyaga omnicopy	Burnt, windfall	
52	52.21100°, 112.53900°	1028	Rhododendron foliage	Burnt, windfall	
53	52.21421°, 112.53182°	1071	Herb foliage	Gorelnic, windfall	
71	52.20604°, 112.55075°	1044	Lingonberry foliage	Burnt, windfall	
72	52.21030°, 112.53596°	1102	Lingonberry foliage	Burnt, windfall	

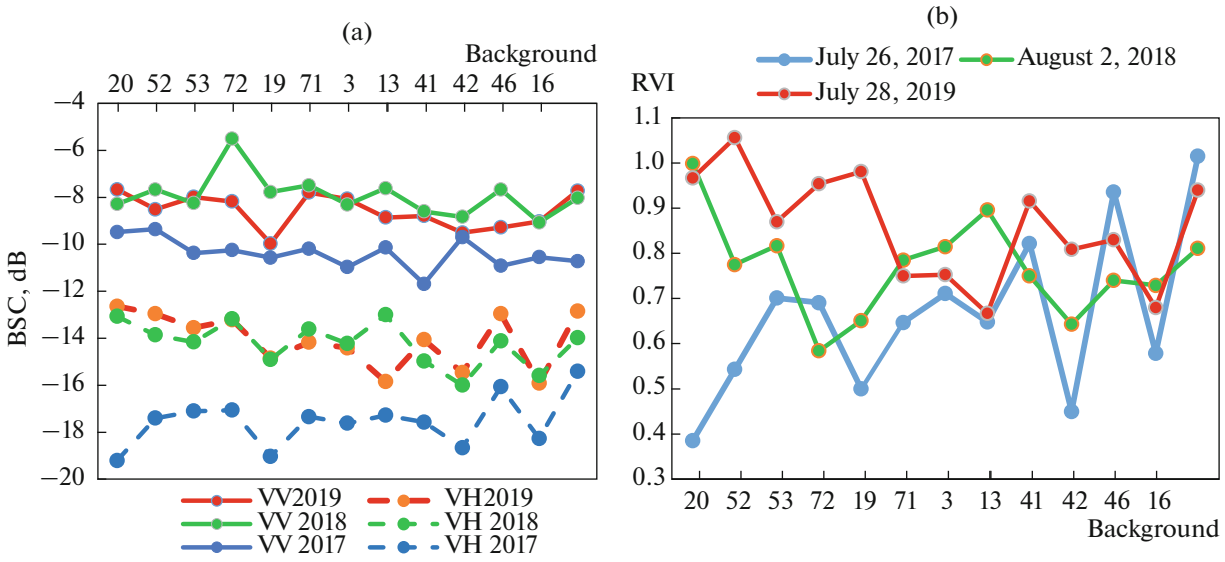

Fig. 3. Changes in (a) the coefficient of backscattering and (b) RVI of test sites for 2017–2019.

two years (i.e., a substantial increase in volume scattering associated with vegetation growth), while it was 1.8 dB for VV polarization. The smallest changes in the BSC of VH polarization were 2.5 dB for the background profile.

The coefficient of backscattering is an absolute polarimetric parameter, while the radar vegetation index (RVI) (Kim and van Zyl, 2004)) is a relative parameter that is not very sensitive to the viewing angle or natural conditions. RVIs are used to monitor the growth of vegetation using multi-temporal radar data:

$$\mathrm{RVI} = \frac{8\sigma_{HV}}{\sigma_{HH} + \sigma_{VV} + 2\sigma_{HV}}. \quad (1)$$

The RVI ranges from 0 (smooth bare soil) to 1 as vegetation grows. It is a measure of volumetric scattering. There are only two polarizations for the Sentinel 1 IW GRD mode: VV and VH. Assuming that $\sigma_{HH} \approx \sigma_{VV}$ (Charbonneau et al., 2005), Eq. (1) can be written as $\mathrm{RVI} = \frac{4\sigma_{VH}}{\sigma_{VV} + \sigma_{VH}}$. This assumption is valid when the interaction between soil and vegetation is negligible (Trudel et al., 2012). The RVI correlates with the volumetric water content (VWC), leaf area index (LAI), and normalized difference vegetation index (NDVI). It is also weakly sensitive to environmental conditions (Kim and van Zyl, 2009). Figure 3b shows a graph of RVI changes for the test sites surveyed on July 26, 2017, August 2, 2018, and July 28, 2019. The greatest RVI growth is typical of sites from group (1), the one farthest north. Note the considerable growth of vegetation for site 20, where the RVI changed from 0.385 in 2017 to 0.99 in 2018. A 6.6 dB increase in the BSC for VH polarization was noted above for the same site. Slightly smaller rises of 0.35 and 0.5 were observed in the RVI for sites 42 and 52, respectively. A decline in the RVI over two years was noted for site 46 and the background site.

Figure 4 shows the images of the studied territory for both polarizations in RGB coding: red is the shooting date July 26, 2017; green is August 2, 2018; and blue is July 28, 2019. All changes on the territory of the burned-out areas observed after the fire in 2015 (indicated on the right side of Fig. 4) occurred in the period 2017–2019. Multi-temporal radar images revealed burned areas, while the rest of the territory changed only slightly.

Initial Sentinel 2 Multispectral Data: Spectral Indices

The Sentinel 2A (S2A) satellite was launched in June 2015, and the Sentinel 2B (S2B) was launched in March 2017. The ESA's S2A and S2B satellites have spatial resolutions (SRs) of 10–60 m, and the frequency of joint surveys is 5 days. The satellites' multispectral cameras have 13 spectral channels: coastal aerosol (B1), three channels of the visible wavelength range (B2, B3, B4), four red-edge channels (B5, B6, B7, and B8a), two channels of the near-infrared range (NIR: B8 and B9), and three SWIR channels (B10, B11, and B12). Images were processed with the SNAP software.

Multispectral sensors are widely used to determine the levels of fire hazard and the post-fire dynamics of vegetation recovery. Spectral channels Red (B4), NIR (B8), and SWIR (B11 and B12) are the ones used most often.

Such spectral indices (SIs) as the NDVI (Normalized Difference Vegetation Index) and VI (Normalized Vegetation Index) (Rouse et al., 1973), and the

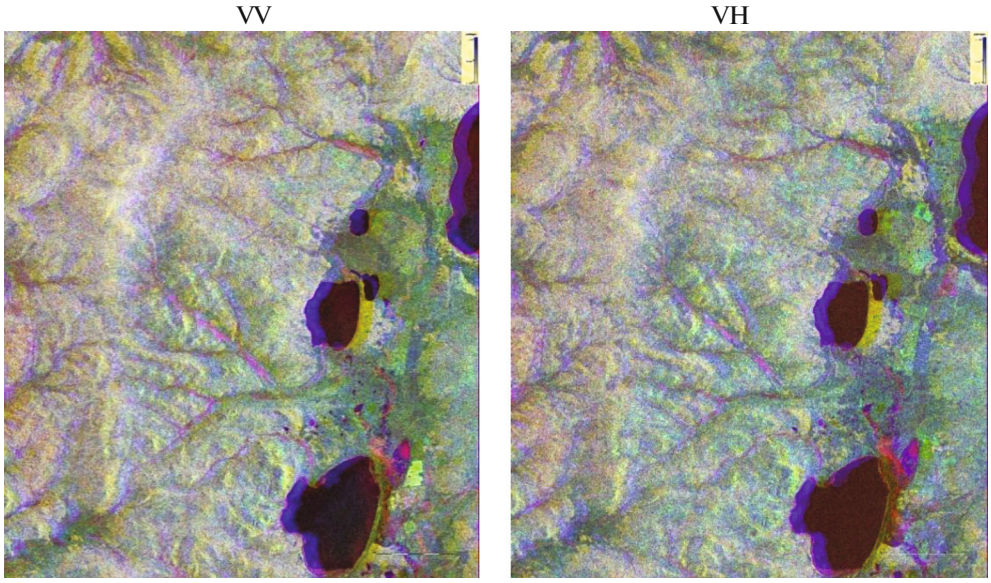

Fig. 4. Images of the studied area in RGB coding: red is July 26, 2017; green is August 2, 2018; blue is July 28, 2019.

NBR (Normalized Burn Ratio) and NBI (Normalized Burning Index) (Key and Benson, 2005)), obtained using optical data from remote sensing, and their modifications the DNDVI (Difference VI) and the DNBR (Difference Burning Index), which determine the difference between indices before and after a fire, produce good results in identifying areas with damage to vegetation cover. Graphs based on the NBR and DNBR indices reflect the dynamics and nature of the restoration of the vegetation cover in burned-out areas (Bondur et al., 2019). It was not possible to use difference indices in this work, since the pre-fire data were from 2014, when the Sentinel 2 survey was not yet available.

Along with the traditionally used NDVI and NBR SIs, the Mid-Infrared Burn Index (MIRBI) (Trigg and Flasse, 2001) and Normalized Difference Red-Edge Index (NDRE) (Barnes et al., 2000) were used in this work to determine the level of vegetation recovery after fires; the formula for the latter includes red-edge channel B6.

S2 images from July 31, 2016, August 5, 2017, July 31, 2018, and July 26, 2019, were used to determine the VI according to profiles for the 12 sites under study. The choice of images was due primarily there being no cloudiness in July and the proximity of the dates to those of the radar survey. Since the territories were covered by clouds or their shadows for a number of sites on July 26, 2019, the data for sites 20, 41, 42, 53, and 72 were replaced with those for July 6, 2019.

The NDVI vegetation index quantifies the presence and state of vegetation (relative biomass) and is determined by the formula $\mathrm{NDVI} = \frac{\mathrm{NIR} - \mathrm{R}}{\mathrm{NIR} + \mathrm{R}}$, where NIR and R are the values of the coefficient of reflection for the Earth's surface in the red and near-infrared ranges of the spectrum. The NDVI ranges from [–1, 1]. Changes in the reflectance in the visible and near-IR spectral regions are associated with the drop in the chlorophyll content in the vegetative organs of drying trees. The absorption band of chlorophyll in the red region of the spectrum (0.65 μm) determines the low level of reflection for vegetation in the visible range. Under stress, the production of chlorophyll in plants slows, reducing its absorption in the visible range and thus raising its reflectivity. In the near-IR range, the coefficient of reflection for green vegetation grows markedly, reaching 45–50% (Bartalev et al., 2010).

Figure 5a shows the graphs of the change in the NDVI for the studied test sites from 2016 to 2019. Interestingly, the NDVI values fell for all sites of group 1 over the years after the fire. One reason for this is a number of disadvantages of the NDVI that lead to uncertainties in its quantitative estimates. Among these are (Huete et al., 2002) nonlinearity, the effect of the atmosphere (water vapor and aerosols), saturation at high values of biomass, sensitivity to the presence of clouds, the effect of soil, the geometry of the site, and the influence of spectral effects (different instruments). The main limitation of the NDVI and similar indices is that optical sensors can monitor only a very thin layer of vegetation and cannot provide information about woody vegetation. The effect atmospheric correction on the quantitative value of SIs, including the NDVI, is described below.

The NBR is determined by the formula (Key et al., 2005)

$$\mathrm{NBR} = \frac{\mathrm{NIR} - \mathrm{SWIR2}}{\mathrm{NIR} + \mathrm{SWIR2}},$$

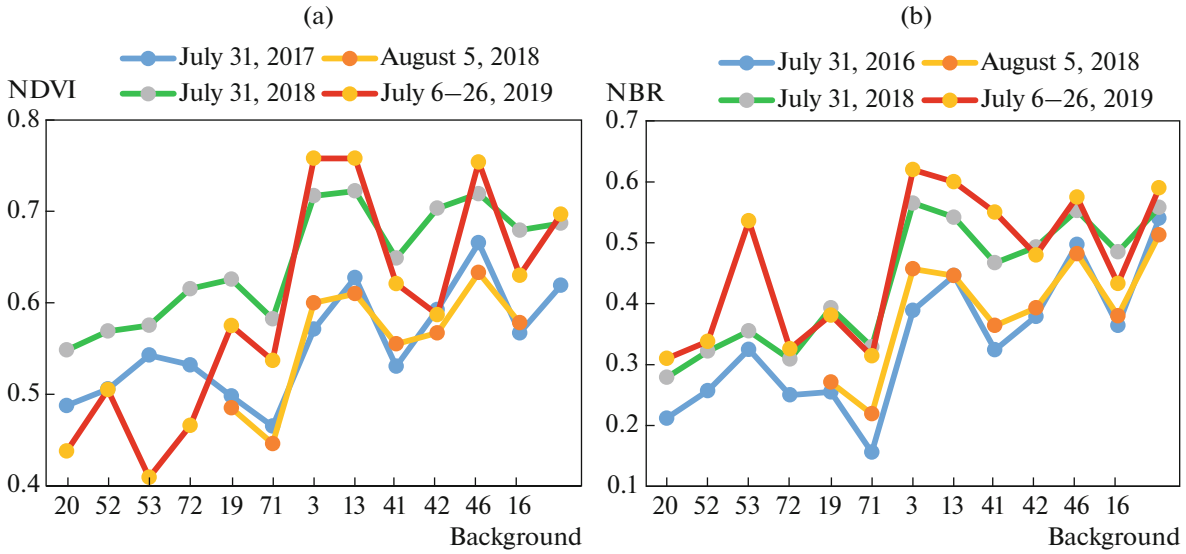

Fig. 5. Changes in the (a) NDVI and (b) NBR at test sites for 2016–2019.

where SWIR2 is the coefficient of reflection for the ground's surface in the mid-IR channel. The central wavelengths are 2.2024 μm (S2A) and 2.1857 μm (S2B) (channel 12, SR = 20 m).

The mid-IR region of the spectrum reflects changes in the moisture content in plants, along with changes in the canopy and leaf structures. Joint use of the mid- and near-IR regions of the spectrum (the latter of which does not depend on the moisture saturation of a plant but on the structure of its leaves) increases the accuracy of determining its moisture content (regardless of the structure of its leaves) (Ceccato et al., 2001).

Figure 5b shows graphs of NBR changes for the considered test sites in the period 2016–2019. These show that the moisture content in plants grew for all test sites exposed earlier to fire while remaining virtually the same for the background site where there was no fire.

The largest increase in the NBR (more than 0.2) was noted for sites 3, 41, and 53. For sites 13 and 71, it was more than 0.15. The smallest change in the NBR (0.05) was noted for the background area.

The joint use of two SIs has been proposed (Trigg and Flasse, 2001) to assess the severity of a fire and the post-fire dynamics of vegetation restoration: MIRBI (Rahman et al., 2019) for the former and NDRE (Barnes et al., 2000) for the latter, where a Red Edge channel is added. It has also been shown (Korets et al., 2010) that VIs based on the Red Edge channel (indicators of the chlorophyll content) are useful for quantifying forest damage due to fire.

The MIRBI spectral index (Trigg and Flasse, 2001) is determined through two SWIR channels. It was found (Trigg and Flasse, 2001) that the combination of these two channels is capable of strong spectral separation of areas exposed to fires but not burned:

$$\mathrm{MIRBI} = 10x\mathrm{SWIR2} - 9.8x\mathrm{SWIR1} + 2.$$

The ability of the MIRBI SI to separate areas with and without burns is shown in Fig. 6a. It did not change the values for the background (area not exposed to fires) for 3 years. For all of the other 12 sites, there is spectral separation according to the level of MIRBI change over 3 years. The largest changes are for sites of the second group (sites 19 and 71), while the slightly smaller changes are for sites 16 and 46. The MIRBI changes are negligible for sites 41 and 52. The severity of the fire for sites of the first group is less than for the sites of the 2nd group.

The NDRE spectral index is determined by the formula (Barnes et al., 2000):

$$\mathrm{NDRE} = \frac{(\mathrm{NIR} - \mathrm{Red\ Edge})}{(\mathrm{NIR} + \mathrm{Red\ Edge})},$$

where Red Edge is channel B6 of Sentinel 2. Figure 6b shows the graphs of changes in the NDRE SI for 13 sites on shooting dates July 31, 2016, July 31, 2018, and July 6–26, 2019. The NDRE values grow for all sites except 46. The greatest increase is noted for site 16 and the sites of group 3.

It is interesting to note the dependence of the SI values on the location latitude, which can be traced from the NDVI and NBR plots in Fig. 5 and the NDRE plot in Fig. 6b. The SI values fall as the geographic latitude of the test site rises. In other words, the vegetation on test sites with more northerly locations was characterized by lower biomass, moisture, and chlorophyll content.

Figure 7 shows a graph of all changes in the absolute value of indices: radar vegetation RVI (2017–2019) and

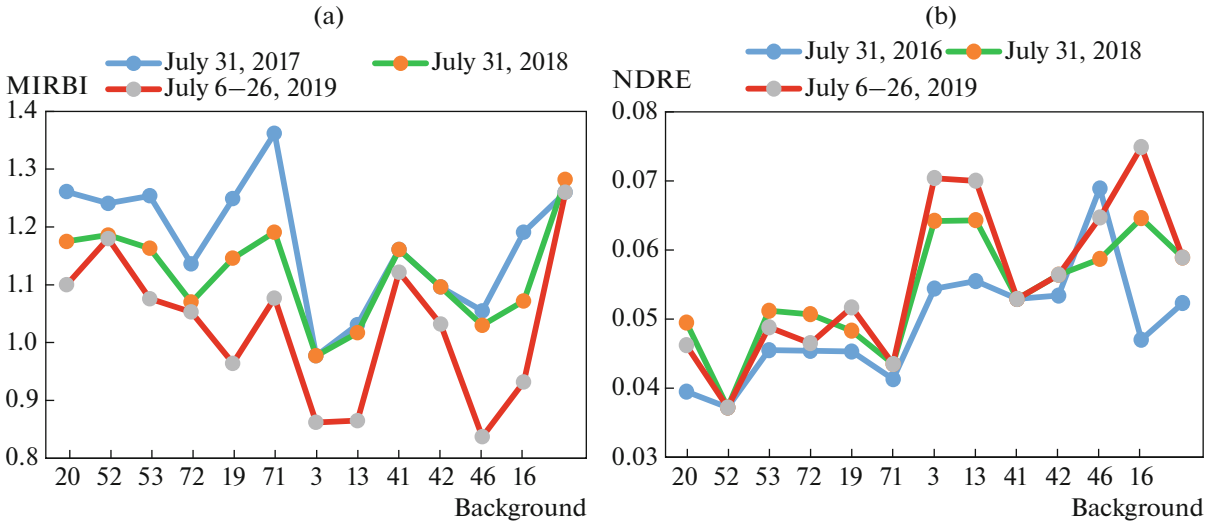

Fig. 6. Changes in the values of MIRBI and NDRE SIs for 2016–2019.

spectral NBR, MIRBI, and NDRE (2016–2019), in the order of placing test sites by groups:

(1) There is a considerable difference between changes in the indices since 2015 for the background and other sites. (The changes are the smallest for the background site.)

(2) The sites of group 1 are distinguished by a strong increase in volumetric dispersion.

(3) The sites of group 2 are distinguished by greater severity of the fire and a considerable increase in volumetric scattering.

(4) The sites of group 3 are distinguished by an increase in the moisture and chlorophyll content of plants at low volumetric scattering.

(5) The sites of group 4 are distinguished by a small change in chlorophyll content, an increase in moisture in the plants, and an increase in volumetric dispersion.

(6) There is a difference between the greater severity of the fire and the largest increase in the chlorophyll content for site 16, compared to other sites.

Based on spectral indices NDVI, NBR, MIRBI, and NDRE, we can draw a general conclusion about the positive dynamics of vegetation recovery after the fire of 2015 at 12 sites on the territory of Ivano–Arakhley Nature Park. Based on the MIRBI index, the greatest severity of the fire was noted for sites of group 2 and then, in declining order, for site 16 and groups 1, 3, and 4. The values of the NBR index, which reflects the moisture in vegetation, and the NDRE index, an indicator of the chlorophyll content, grew over the post-fire years for all test sites. Based on the RVI radar vegetation index, an increase in the volumetric scattering associated with vegetation growth was shown for all sites (more for group 1, and in declining order for groups 2 and 4).

The importance of the integrated use of optical and radar data for remote sensing of forest areas was thus demonstrated (Bondur and Chimitdorzhiev, 2008).

Effect of Atmospheric Correction on the Values of Spectral Indices

Each beam passes through the atmosphere twice before reaching the satellite's sensor. The atmospheric effect on the signal is due to scattering by aerosol particles and gas molecules, and to absorption by gases. Data from the Sentinel 2 imaging system are provided

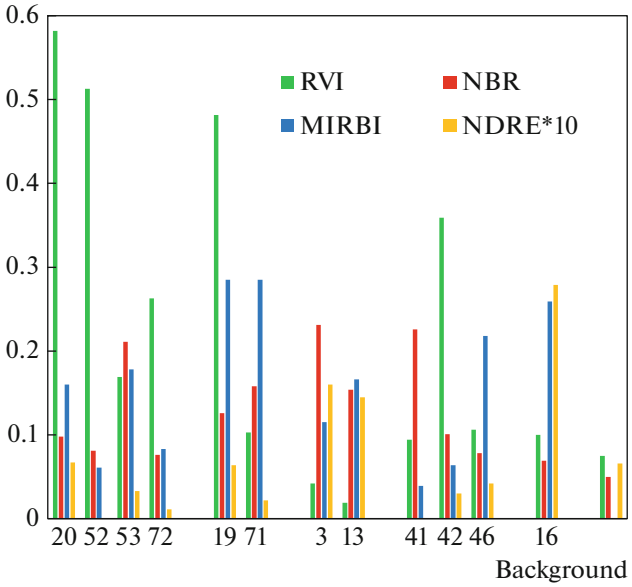

Fig. 7. Changes in the absolute values of the vegetation radar and spectral indices for the studied sites.

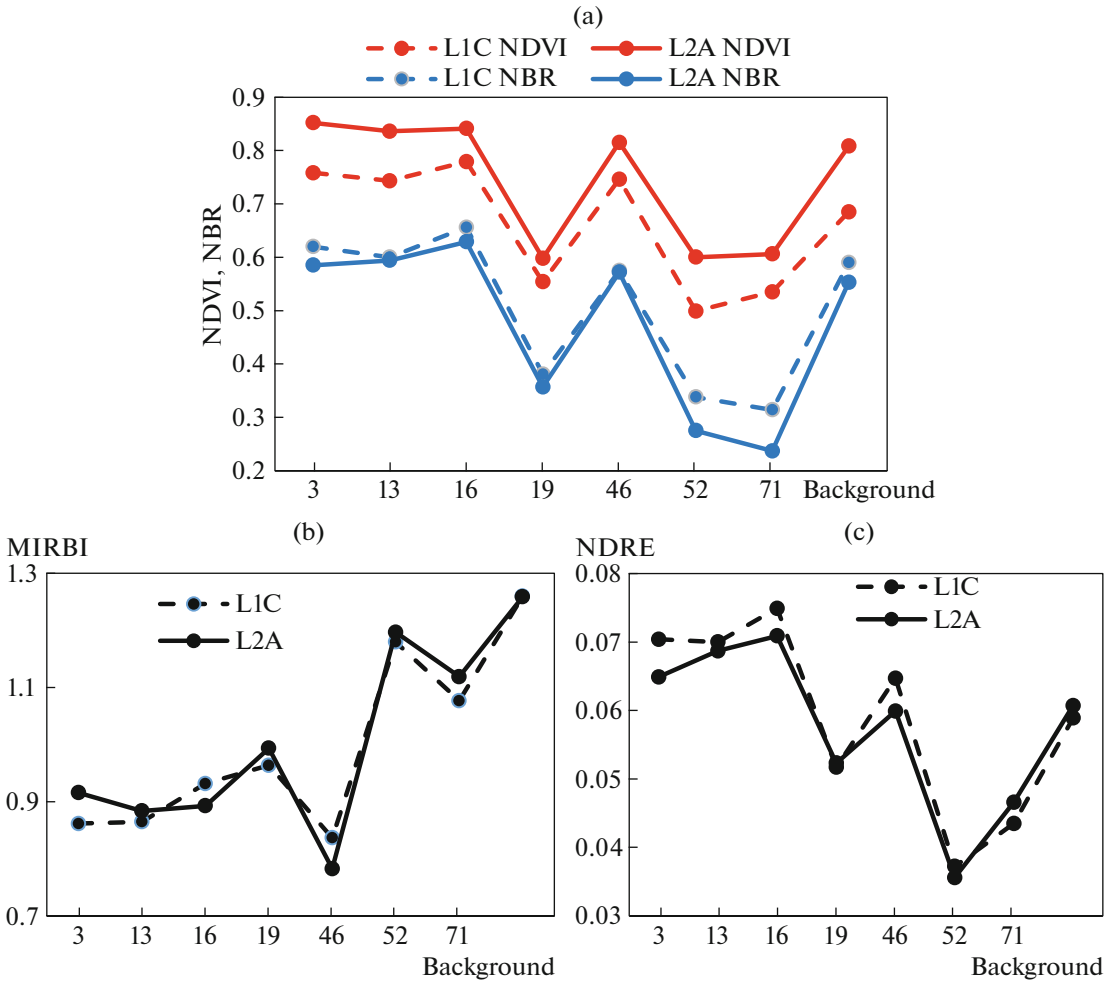

Fig. 8. (a) NDVI and NBR, (b) MIRBI, and (c) NDRE SI values before and after atmospheric correction.

to the user with L1C processing in the form of the albedo at the top of the atmosphere (TOA, Top-of-Atmosphere Reflectance) with radiometric and geometric corrections. These data can be processed to the L2A level in the form of the albedo at the lower boundary of the atmosphere (BOA, Bottom-of-Atmosphere) using the free atmospheric correction program Sen2Cor.

We can see how the SI values considered in this work changed after atmospheric correction (AC). Figure 8 shows the plots of NDVI, NBR, MIRBI, and NDRE values before and after AC for some sites on July 26, 2019 (this was not possible for all sites, due to clouds being in the S2 images). The graphs for the NDVI and NBR (Fig. 8a) show that of these two SIs, AC had a stronger effect on the NDVI, which after AC raised their values by more than 10% for individual sites (3, 13, 52, and background). AC had a much weaker effect on the NBR SI. NBR SI values remained virtually the same for all sites after AC, except for 52 and 71, while the quantitative values fell. As with the NBR, AC had a negligible effect on the numerical values of the MIRBI and NDRE SIs (Figs. 8b, 8c). We may therefore conclude the atmospheric stability of spectral indices NBR, MIRBI, NDRE was greater than that of the NDVI.

Figure 9 shows two S2 images of the studied territory (Shakshinskoe Lake is in the lower right corner) on July 26, 2019, in natural colors, using a combination of channels B2, B3, and B4 before (Fig. 9a) and after (Fig. 9b) atmospheric correction. The size of the image is 1407 × 1159 pixels.

CONCLUSIONS

We determined the dynamics of vegetation restoration on the territory of Ivano–Arakhley Nature Park after wildfires in April 2015, using radar and optical data from Sentinel satellites 1 and 2. Spectral indices NDVI, NBR, MIRBI, NDRE and radar vegetation index RVI showed positive dynamics in the state of vegetation at 12 test sites over the years after the fire (2016–2019) through an increase in the values of the NDVI, NBR, NDRE, RVI vegetation indices. It was

Fig. 9. Comparison of two S2 images in natural colors (channels B2, B3, B4) taken on July 26, 2019, (a) before and (b) after atmospheric correction.

shown that the values of vegetation indices rose as the latitudes of the sites fell, and the spectral indices NBR, MIRBI, and NDRE had higher atmospheric stability of the SI used to estimate the severity of the fire and postfire restoration of vegetation than that of the NDVI.

ACKNOWLEDGMENTS

The authors thank V.P. Makarov, Candidate of Biological Sciences and Senior Fellow at the Institute of Natural Resources, Ecology, and Cryology's Laboratory of Geography and Regional Nature Management, for organizing our field work in the area of the Beklemishevskaya Depression.

FUNDING

The work was performed as part of State Task no. 0030-2019-0008 ("Space").

REFERENCES

Barnes, E.M., Clarke, T.R., Richards, S.E., Colaizzi, P.D., Haberland, J., Kostrzewski, M., Waller, P., Choi, C., Riley, E., Thompson, T., Lascano, R.J., Li, H., and Moran, M.S., Coincident detection of crop water stress, nitrogen status and canopy density using ground-based multispectral data, in *Proceedings of the Fifth International Conference on Precision Agriculture*, Madison, Wis.: ASA-CSSA-SSSA, 2000.

Bartalev, S.A., Egorov, V.A., Krylovi, A.M., Stytsenko, F.V., and Khovratovich, T.S., Possibilities to assess the state of burnt forests with the help of multispectral satellite data, *Sovrem. Probl. Distantsionnogo Zondirovaniya Zemli Kosmosa*, 2010, no. 7, pp. 215–225.

Bondur, V.G. and Chimitdorzhiev, T.N., Remote sensing of vegetation by optical microwave methods, *Izv. Vyssh. Uchebn. Zaved., Geod. Aerofotos'emka*, 2008, no. 6, pp. 64–73.

Bondur, V.G., Tsidilina, M.N., and Cherepanova, E.V., Satellite monitoring of wildfire impacts on the conditions of various types of vegetation cover in the federal districts of the Russian Federation, *Izv., Atmos. Ocean. Phys.*, 2019, vol. 55, no. 9, pp. 1238–1253.

Ceccato, P., Flasse, S., Tarantola, S., Jacquemond, S., and Gregoire, J., Detecting vegetation water content using reflectance in the optical domain, *Remote Sens. Environ.*, 2001, pp. 22–33.

Charbonneau, F., Trudel, M., and Fernandes, R., Use of dual polarization and multi-incidence SAR for soil permeability mapping, in *Advanced Synthetic Aperture Radar (ASAR)*, St. Hubert, Canada, 2005.

Gorbunov, I.V., Makarov, V.P., and Malykh, O.F., Postfire vegetation state in the Ivano-Arakhlei natural park (Zabaikalskii krai), *Usp. Sovrem. Estestvozn.*, 2015, no. 7, pp. 54–59.

Huete, A., Didan, K., and Miura, T., Overview of the radiometric and biophysical performance of the MODIS vegetation indices, *Remote Sens. Environ.*, 2002, vol. 83, no. 195, pp. 213–221.

Key, C.H. and Benson, N.C., Landscape assessment: Ground measure of severity, the Composite Burn Index; and remote sensing of severity, the *Normalized Burn Ratio, in FIREMON: Fire Effects Monitoring and Inventory System*, Lutes, D.C., Keane, R.E., Caratti, J.F., et al., Eds., Ogden, Utah: USDA Forest Service, Rocky Mountain Research Station, 2005, General Technical Report RMRS-GTR-164-CD.

Kim, Y. and van Zyl, J., Vegetation effects on soil moisture estimation, in *Proc. Int. Conf. IEEE Geoscience and Remote Sensing Society (IGARSS)*, 2004, vol. 2, pp. 800–802.

Kim, Y. and van Zyl, J., A time-series approach to estimate soil moisture using polarimetric radar data, *IEEE Trans. Geosci. Remote Sens.*, 2009, vol. 47, no. 8, pp. 2519–2527.

Korets, M.A., Ryzhkova, V.A., Danilova, I.V., Sukhinin, A.I., and Bartalev, S.A., Forest disturbance assessment using satellite data for moderate and low resolution, in *Environment Change in Siberia: Earth Observation. Field Studies and Modeling*, Balzter, H., Ed., Springer, 2010.

Rahman, Sh., Chang, H.-Ch., Magill, Ch., Tomkins, K., and Hehir, W., Spatio–temporal assessment of fire severity and vegetation recovery utilizing SENTINEL-2 imagery in New South Wales, Australia, in *Proc. Int. Conf. IEEE Geoscience and Remote Sensing Society (IGARSS)*, 2019, pp. 9960–9963.

Rodionova, N.V., Evaluation of Sentinel 1 imagery for burned area detection in southern Siberia in spring and summer 2015, *Sovrem. Probl. Distantsionnogo Zondirovaniya Zemli Kosmosa*, 2016, vol. 13, no. 2, pp. 164–175.

Rouse, J.W., Haas, R.H., Schell, J.A., and Deering, D.W., Monitoring vegetation systems in the Great Plains with ERTS, in *Third ERTS Symposium, NASA SP-351 I*, 1973, pp. 309–317.

Shvetsov, E.G., Kukavskaya, E.A., Buryak, L.V., and Barrett, K., Assessment of post-fire vegetation recovery in Southern Siberia using remote sensing observations, *Environ. Res. Lett.*, 2019, vol. 14, pp. 1–10. https://doi.org/10.1088/1748-9326/ab083d

Trigg, S. and Flasse, S., An evaluation of different bi-spectral spaces for discriminating burned shrub-savannah, *Int. J. Remote Sens.*, 2001, vol. 22, no. 13, pp. 2641–2647.

Trudel, M., Charbonneau, F., and Leconte, R., Using RADARSAT-2 polarimetric and ENVISAT-ASAR dual-polarization data for estimating soil moisture over agricultural fields, *Can. J. Remote Sens.*, 2012, vol. 38, no. 4, pp. 514–527.

Translated by A. Ivanov